Probing Ion/Molecule Interactions in Aqueous Solutions with Vibrational Energy Transfer

Jiebo Li, Hongtao Bian, Xiewen Wen, Hailong Chen, Kaijun Yuan, Junrong Zheng*

Department of Chemistry, Rice University, Houston, TX 77005

Supporting materials

This file includes:

Supporting material text

Figure S1 to S17

Table S1 to S5

References

Kinetic model and fitting results

In a KSCN-amino acid -water solution, there are three types of thiocyanate anions: clustered, hydrated (free) and amino acid-complexed. The latter two are considered as the isolated species in the kinetic model, because the vibrational energy transfer among the anions of the isolated species is much slower than that of the clustered under the assumption of dipole-dipole approximation. Based on the physical picture, a kinetic model was constructed to quantitatively analyze the experiments. As shown in Scheme S1, the vibrational excitations of all species decay with their own lifetimes. The clustered anions can exchange their vibrational excitations. At room temperature, the clustered ions and the isolated ions are under dynamic equilibrium[1].

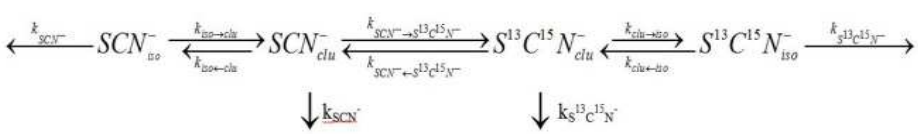

Scheme S1.

From the model, four differential equations are derived as below:

$$\frac{d\left[SCN^-_{clu}(t)^*\right]}{dt}=k_{iso\to clu}\left[SCN^-_{iso}(t)^*\right]+k_{SCN^-\leftarrow S^{13}C^{15}N^-}\left[S^{13}C^{15}N^-_{clu}(t)^*\right]-\left(k_{iso\leftarrow clu}+k_{SCN^-\to S^{13}C^{15}N^-}+k_{SCN^-}\right)\left[SCN^-_{clu}(t)^*\right] \quad \text{Eq. S1}$$

$$\frac{d\left[SCN^-_{iso}(t)^*\right]}{dt}=k_{iso\leftarrow clu}\left[SCN^-_{clu}(t)^*\right]-\left(k_{SCN^-}+k_{iso\to clu}\right)\left[SCN^-_{iso}(t)^*\right] \quad \text{Eq. S2}$$

$$\frac{d\left[S^{13}C^{15}N^-_{clu}(t)^*\right]}{dt}=k_{iso\to clu}\left[S^{13}C^{15}N^-_{iso}(t)^*\right]+k_{SCN^-\to S^{13}C^{15}N^-}\left[SCN^-_{clu}(t)^*\right]-\left(k_{iso\leftarrow clu}+k_{SCN^-\leftarrow S^{13}C^{15}N^-}+k_{S^{13}C^{15}N^-}\right)\left[S^{13}C^{15}N^-_{clu}(t)^*\right] \quad \text{Eq. S3}$$

$$\frac{d\left[S^{13}C^{15}N^-_{iso}(t)^*\right]}{dt}=k_{iso\leftarrow clu}\left[S^{13}C^{15}N^-_{clu}(t)^*\right]-\left(k_{S^{13}C^{15}N^-}+k_{iso\to clu}\right)\left[S^{13}C^{15}N^-_{iso}(t)^*\right] \quad \text{Eq. S4}$$

The time dependent populations (isolated SCN^-, clustering SCN, isolated $S^{13}C^{15}N^-$ and clustering $S^{13}C^{15}N^-$) and vibrational lifetimes are experimentally determined. The isolated and clustered species equilibrium constant K ($K = \frac{k_{iso \to clu}}{k_{iso \leftarrow clu}}$) determine the location exchange rate constant ratio. The energy exchange rate constant ratio D is determined by the energy mismatch of the two vibrations. The normalized initial populations are: $\left[SCN^-_{clu}(0)^*\right] = \frac{K}{K+1}$, $\left[SCN^-_{iso}(0)^*\right] = \frac{1}{K+1}$, $\left[S^{13}C^{15}N^-_{clu}(0)^*\right] = \left[S^{13}C^{15}N^-_{iso}(0)^*\right] = 0$. Solving equations (Eq. (S1) ~Eq. (S4)) with our experiment results gives the energy transfer rate constants, the isolated-clustered ion equilibrium constant ($k_{iso \to clu}$ and $k_{iso \leftarrow clu}$) and the isolated/clustered equilibrium constant (K).

For the solutions, the ideal detailed balance of peak 6 and peak 8 is 0.7 due to the energy mismatch 73 cm^{-1}. This can be easily obtained from experiments as the intensity ratio of peak 8 to peak 6 is 0.7. Therefore, D is a constant. Our previous experiments[2] show that from 4M KSCN aqueous solution to 1.8M solution, the cluster ratio decreases from 67% to 35%. However, the average cluster size remains almost constant (5 to 4). In solutions A~O, most of the cluster ratios are within this range. Therefore, we assume that the cluster size is constant in all solutions so that we can keep the energy transfer rate constants constant for all samples in the calculations to have a fair comparison for the cluster ratios.

Analysis based on experimental results and the kinetic model for solution A gives $k_{SCN^- \to S^{13}C^{15}N^-} = 1/140\ (ps^{-1})$. Equilibrium constant K is 2.0, which indicates that the cluster ratio is 67%. The location exchange rate constant is $k_{clu \to iso} = 1/10\ (ps^{-1})$.

Experimental results and calculations based on the kinetic model with the following parameters are displayed in Figure S1:

$k_{SCN^-fast} = 1/3.1\ (ps^{-1})$; $k_{SCN^-slow} = 1/30.5\ (ps^{-1})$; $k_{S^{13}C^{15}N^-fast} = 1/2.1\ (ps^{-1})$; $k_{S^{13}C^{15}N^-slow} = 1/25.1\ (ps^{-1})$;
$k_{clu\to iso} = 1/10\ (ps^{-1})$; K=2.0; $k_{SCN^-\to S^{13}C^{15}N^-} = 1/140\ (ps^{-1})$; D=0.7

with pre-factors of the subgroups and offset of the bi-exponential

$A_{SCN^-fast} = 0.05$; $A_{SCN^-slow} = 0.95$; $A_{S^{13}C^{15}N^-fast} = 0.07$; $A_{S^{13}C^{15}N^-slow} = 0.93$; $offset = 0$.

For solutions B~O, calculations and experimental results are displayed in Figure S2~S14. Parameters for calculations are listed in the following. Here it is necessary to note that in our experiment, the cross peaks and the diagonal peaks are measured in different laser focusing conditions. For the cross peak measurement, the pump laser beam was focused very tight at the sample because the energy transfer peaks are usually very weak, especially when the amino acids were added to the KSCN/$KS^{13}C^{15}N$ solution. Also we only measured the cross peaks when the pump located at 2060 cm^{-1} and peak 6 was used to do the energy transfer analysis. While the other cross peaks pair (peak 7 and peak 8) are not measured. Since we already know the detailed balance ratio for the pumping/up and flowing down is 0.7 for the KSCN/$KS^{13}C^{15}N$ solution, we simply scaled the flowing down curves by 0.7 as the pumping up curves in our data analysis. However we cannot use the diagonal peaks to do the vibrational lifetime analysis when the pump laser beam was tightly focused, because high order nonlinear processes may occur for the KSCN solution which may affect the vibrational lifetime analysis. Alternatively, for the vibrational lifetime analysis, we defocused the pump laser beam to eliminate the high order nonlinear processes and the generated pump probe signals are significantly attenuated.

For solution B, the calculation parameters are:

$k_{SCN^-fast} = 1/1.5(ps^{-1})$; $k_{SCN^-slow} = 1/14.5\ (ps^{-1})$; $k_{S^{13}C^{15}N^-fast} = 1/1.1\ (ps^{-1})$; $k_{S^{13}C^{15}N^-slow} = 1/15.0\ (ps^{-1})$;
$k_{clu\to iso} = 1/10\ (ps^{-1})$; K=0.92; $k_{SCN^-\to S^{13}C^{15}N^-} = 1/140\ (ps^{-1})$; D=0.7

with pre-factors of the subgroups and offset of the single-exponential

$A_{SCN^-fast} = 0.15;\ A_{SCN^-slow} = 0.85;\ A_{S^{13}C^{15}N^-fast} = 0.10;\ A_{S^{13}C^{15}N^-slow} = 0.90;\ offset = 0$

Solution C:

$k_{SCN^-fast} = 1/2.5\ (ps^{-1})$; $k_{SCN^-slow} = 1/15.3\ (ps^{-1})$; $k_{S^{13}C^{15}N^-fast} = 1/2.1\ (ps^{-1})$; $k_{S^{13}C^{15}N^-slow} = 1/16.5\ (ps^{-1})$;
$k_{clu\to iso} = 1/6\ (ps^{-1})$; K=0.51; $k_{SCN^-\to S^{13}C^{15}N^-} = 1/140\ (ps^{-1})$; D=0.7

with pre-factors of the subgroups and offset of the bi-exponential

$A_{SCN^-fast} = 0.08;\ A_{SCN^-slow} = 0.92;\ A_{S^{13}C^{15}N^-fast} = 0.15;\ A_{S^{13}C^{15}N^-slow} = 0.85;\ offset = 0$ ·

Solution D:

$k_{SCN^-fast} = 1/1.26(ps^{-1})$; $k_{SCN^-slow} = 1/14.2\ (ps^{-1})$; $k_{S^{13}C^{15}N^-fast} = 1/1.3\ (ps^{-1})$; $k_{S^{13}C^{15}N^-slow} = 1/18.0\ (ps^{-1})$;
$k_{clu\to iso} = 1/10\ (ps^{-1})$; K=0.82; $k_{SCN^-\to S^{13}C^{15}N^-} = 1/140\ (ps^{-1})$; D=0.7

with pre-factors of the subgroups and offset of the bi-exponential

$A_{SCN^-fast} = 0.085;\ A_{SCN^-slow} = 0.915;\ A_{S^{13}C^{15}N^-fast} = 0.116;\ A_{S^{13}C^{15}N^-slow} = 0.884;\ offset = 0$ ·

Solution E:

$k_{SCN^-fast} = 1/1.7(ps^{-1})$; $k_{SCN^-slow} = 1/16.5\ (ps^{-1})$; $k_{S^{13}C^{15}N^-fast} = 1/2.6\ (ps^{-1})$; $k_{S^{13}C^{15}N^-slow} = 1/17.8\ (ps^{-1})$;
$k_{clu\to iso} = 1/10\ (ps^{-1})$; K=0.60; $k_{SCN^-\to S^{13}C^{15}N^-} = 1/145\ (ps^{-1})$; D=0.7

with pre-factors of the subgroups and offset of the bi-exponential

$A_{SCN^-fast} = 0.04;\ A_{SCN^-slow} = 0.96;\ A_{S^{13}C^{15}N^-fast} = 0.17;\ A_{S^{13}C^{15}N^-slow} = 0.83;\ offset = 0$

Solution F

$k_{SCN^-fast} = 1/1.26(ps^{-1})$; $k_{SCN^-slow} = 1/13.0\ (ps^{-1})$; $k_{S^{13}C^{15}N^-fast} = 1/1.30\ (ps^{-1})$; $k_{S^{13}C^{15}N^-slow} = 1/13.1\ (ps^{-1})$;
$k_{clu\to iso} = 1/10\ (ps^{-1})$; K=0.42; $k_{SCN^-\to S^{13}C^{15}N^-} = 1/140\ (ps^{-1})$; D=0.7

with pre-factors of the subgroups and offset of the bi-exponential

$A_{SCN^-fast} = 0.085;\ A_{SCN^-slow} = 0.915;\ A_{S^{13}C^{15}N^-fast} = 0.116;\ A_{S^{13}C^{15}N^-slow} = 0.884;\ offset = 0$

Solution G:

$k_{SCN^-fast} = 1/1.75 (ps^{-1})$; $k_{SCN^-slow} = 1/31.56\ (ps^{-1})$; $k_{S^{13}C^{15}N^-fast} = 1/2.11\ (ps^{-1})$; $k_{S^{13}C^{15}N^-slow} = 1/34.45\ (ps^{-1})$;
$k_{clu\to iso} = 1/10\ (ps^{-1})$; K=1.85; $k_{SCN^-\to S^{13}C^{15}N^-} = 1/140\ (ps^{-1})$; D=0.7

with pre-factors of the subgroups and offset of the bi-exponential

$A_{SCN^-fast} = 0.085;\ A_{SCN^-slow} = 0.915;\ A_{S^{13}C^{15}N^-fast} = 0.116;\ A_{S^{13}C^{15}N^-slow} = 0.884;\ offset = 0$

Solution H:

$k_{SCN^-fast} = 0 (ps^{-1})$;$k_{SCN^-slow} = 1/17.2\ (ps^{-1})$; $k_{S^{13}C^{15}N^-fast} = 0 (ps^{-1})$; $k_{S^{13}C^{15}N^-slow} = 1/16.2 (ps^{-1})$;
$k_{clu\to iso} = 1/10\ (ps^{-1})$; K=0.85; $k_{SCN^-\to S^{13}C^{15}N^-} = 1/140\ (ps^{-1})$; D=0.7

with pre-factors of the subgroups and offset of the bi-exponential

$A_{SCN^-fast} = 0.0;\ A_{SCN^-slow} = 1;\ A_{S^{13}C^{15}N^-fast} = 0;\ A_{S^{13}C^{15}N^-slow} = 1;\ offset = 0$

Solution J:

$k_{SCN^-fast} = 1/4.5\ (ps^{-1})$; $k_{SCN^-slow} = 1/26.0\ (ps^{-1})$; $k_{S^{13}C^{15}N^-fast} = 1/4.0\ (ps^{-1})$; $k_{S^{13}C^{15}N^-slow} = 1/27.5\ (ps^{-1})$;
$k_{clu\to iso} = 1/10\ (ps^{-1})$; K=1.28; $k_{SCN^-\to S^{13}C^{15}N^-} = 1/140\ (ps^{-1})$; D=0.7

with pre-factors of the subgroups and offset of the bi-exponential

$A_{SCN^-fast} = 0.12;\ A_{SCN^-slow} = 0.88;\ A_{S^{13}C^{15}N^-fast} = 0.08;\ A_{S^{13}C^{15}N^-slow} = 0.92;\ offset = 0$

Solution K:

$k_{SCN^-fast} = 1/1.26 (ps^{-1})$; $k_{SCN^-slow} = 1/22.90\ (ps^{-1})$; $k_{S^{13}C^{15}N^-fast} = 1/1.3\ (ps^{-1})$; $k_{S^{13}C^{15}N^-slow} = 1/23.25\ (ps^{-1})$;
$k_{clu\to iso} = 1/10\ (ps^{-1})$; K=1.0; $k_{SCN^-\to S^{13}C^{15}N^-} = 1/140\ (ps^{-1})$; D=0.7

with pre-factors of the subgroups and offset of the bi-exponential

$A_{SCN^-fast} = 0.085;\ A_{SCN^-slow} = 0.915;\ A_{S^{13}C^{15}N^-fast} = 0.126;\ A_{S^{13}C^{15}N^-slow} = 0.874;\ offset = 0$

Solution L:

$k_{SCN^-fast} = 1/1.26\ (ps^{-1})$; $k_{SCN^-slow} = 1/21.90\ (ps^{-1})$; $k_{S^{13}C^{15}N^-fast} = 1/1.3\ (ps^{-1})$; $k_{S^{13}C^{15}N^-slow} = 1/29.0\ (ps^{-1})$;
$k_{clu\to iso} = 1/10\ (ps^{-1})$; K=1.74; $k_{SCN^-\to S^{13}C^{15}N^-} = 1/140\ (ps^{-1})$; D=0.7

with pre-factors of the subgroups and offset of the bi-exponential

$A_{SCN^-fast} = 0.085;\ A_{SCN^-slow} = 0.915;\ A_{S^{13}C^{15}N^-fast} = 0.116;\ A_{S^{13}C^{15}N^-slow} = 0.884;\ offset = 0$

Solution M:

$k_{SCN^-fast} = 1/1.26\ (ps^{-1})$; $k_{SCN^-slow} = 1/28.00\ (ps^{-1})$; $k_{S^{13}C^{15}N^-fast} = 1/1.3\ (ps^{-1})$; $k_{S^{13}C^{15}N^-slow} = 1/33.0\ (ps^{-1})$;
$k_{clu\to iso} = 1/10\ (ps^{-1})$; K=1.52; $k_{SCN^-\to S^{13}C^{15}N^-} = 1/140\ (ps^{-1})$; D=0.7

with pre-factors of the subgroups and offset of the bi-exponential

$A_{SCN^-fast} = 0.085;\ A_{SCN^-slow} = 0.915;\ A_{S^{13}C^{15}N^-fast} = 0.116;\ A_{S^{13}C^{15}N^-slow} = 0.884;\ offset = 0$

Solution N:

$k_{SCN^-slow} = 1/20\ (ps^{-1});\ k_{S^{13}C^{15}N^-slow} = 1/24.8\ (ps^{-1});$
$k_{clu\to iso} = 1/10\ (ps^{-1});$ K=1.05; $k_{SCN^-\to S^{13}C^{15}N^-} = 1/140.0\ (ps^{-1});$

with pre-factors of the subgroups and offset of the bi-exponential

$A_{SCN^-fast} = 0.0;\ A_{SCN^-slow} = 1;\ A_{S^{13}C^{15}N^-fast} = 0.0;\ A_{S^{13}C^{15}N^-slow} = 1.0;\ offset = 0$

Solution O:

$k_{SCN^-fast} = 1/2.9(ps^{-1});\ k_{SCN^-slow} = 1/19.70(ps^{-1});\ k_{S^{13}C^{15}N^-fast} = 1/1.80\ (ps^{-1});\ k_{S^{13}C^{15}N^-slow} = 1/21.98\ (ps^{-1});$
$k_{clu\to iso} = 1/10\ (ps^{-1});$ K=1.10; $k_{SCN^-\to S^{13}C^{15}N^-} = 1/140\ (ps^{-1});$ D=0.7

with pre-factors of the subgroups and offset of the bi-exponential

$A_{SCN^-fast} = 0.10;\ A_{SCN^-slow} = 0.90;\ A_{S^{13}C^{15}N^-fast} = 0.14;\ A_{S^{13}C^{15}N^-slow} = 0.86;\ offset = 0$

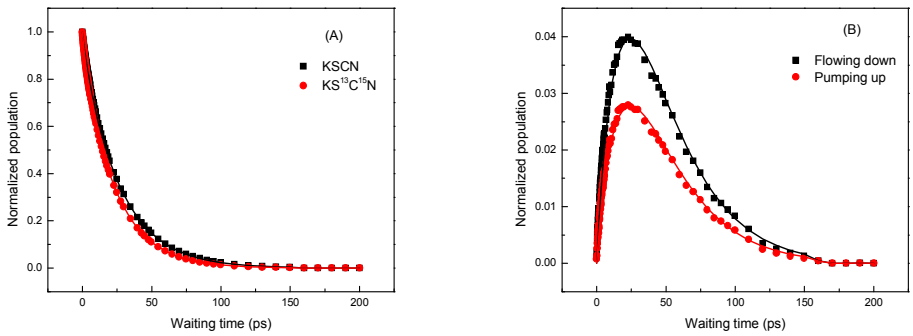

Figure S1. Data and calculations of **Solution A** (4.0M KSCN/$KS^{13}C^{15}N$ D_2O solution); Dots are data, and lines are calculations.

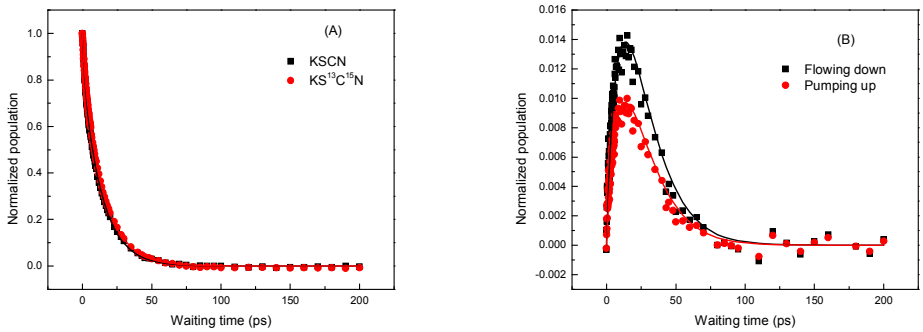

Figure S2. Data and calculations of **Solution B** (Pro:KSCN:$KS^{13}C^{15}N$:D_2O =1:1:1:20). Dots are data, and lines are calculations

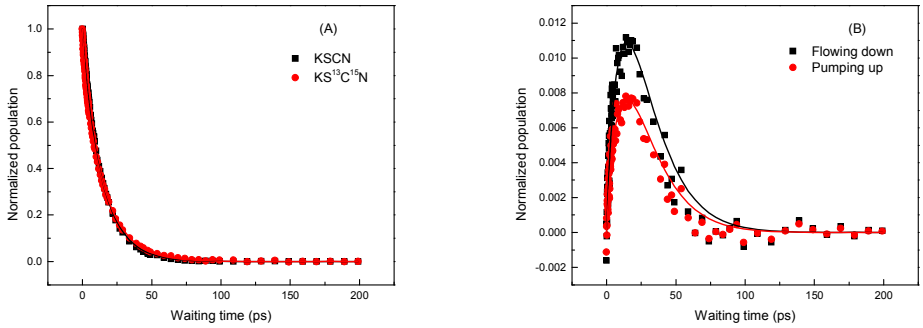

Figure S3. Data and calculations of **Solution C** (Pro:KSCN:$KS^{13}C^{15}N$:D_2O =2:1:1:20). Dots are data, and lines are calculations

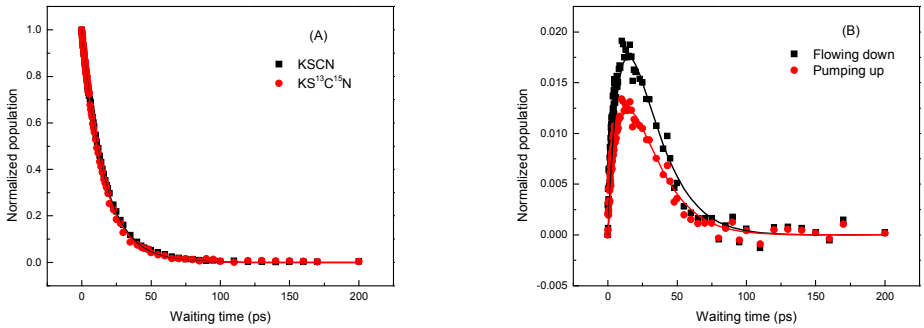

Figure S4. Data and calculations of **Solution D** (Gly:KSCN:$KS^{13}C^{15}N$:D_2O=1:1:1:20). Dots are data, and lines are calculations.

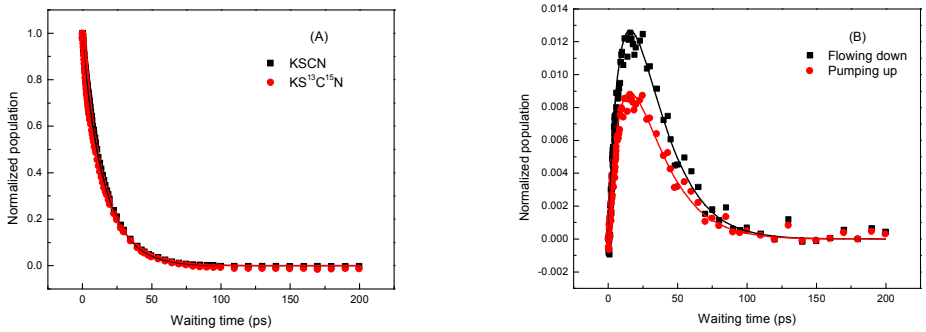

Figure S5. Data and calculations of **Solution E** (Cys:KSCN:$KS^{13}C^{15}N$:D_2O =1:1:1:20). Dots are data, and lines are calculations.

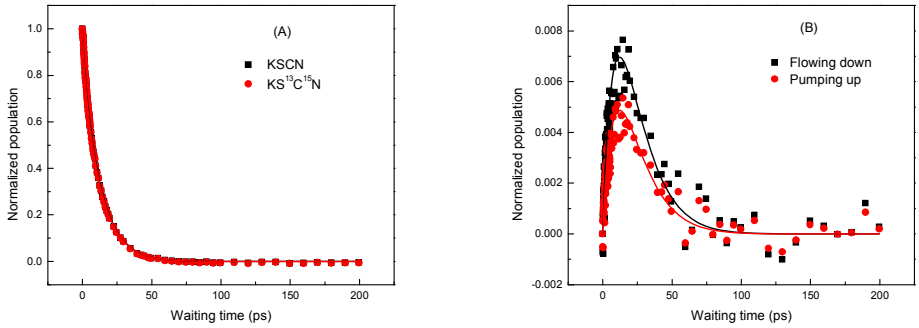

Figure S6. Data and calculations of **Solution F** (Lys:KSCN:$KS^{13}C^{15}N$:D_2O =1:1:1:20). Dots are data, and lines are calculations.

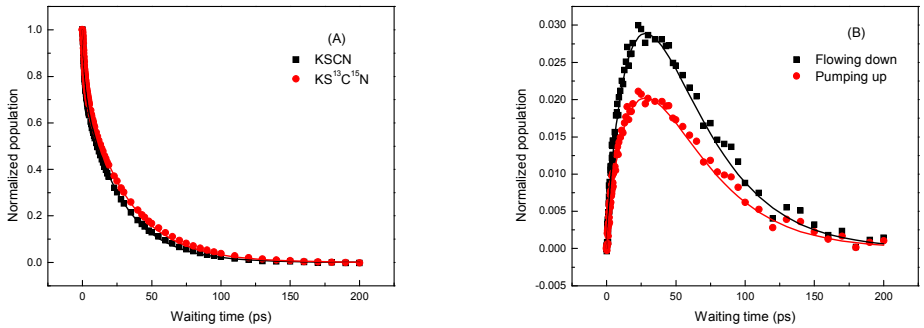

Figure S7. Data and calculations of **Solution G** (CH_3COOK:KSCN:$KS^{13}C^{15}N$:D_2O =2:1:1:20). Dots are data, and lines are calculations.

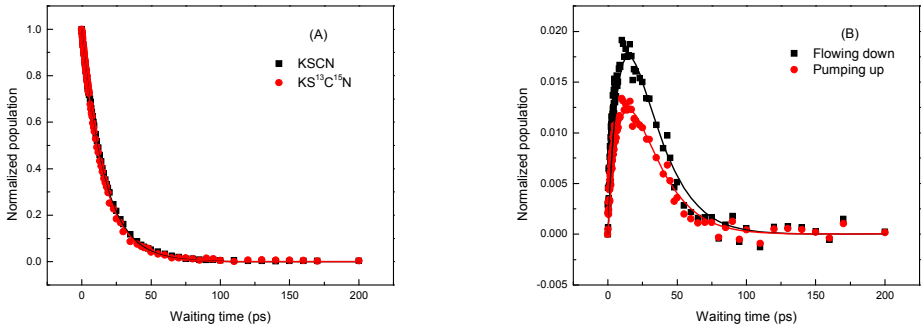

Figure S8. Data and calculations of **Solution H** (CH_3NH_3Cl:KSCN:$KS^{13}C^{15}N$:D_2O =1:1:1:20). Dots are data, and lines are calculations.

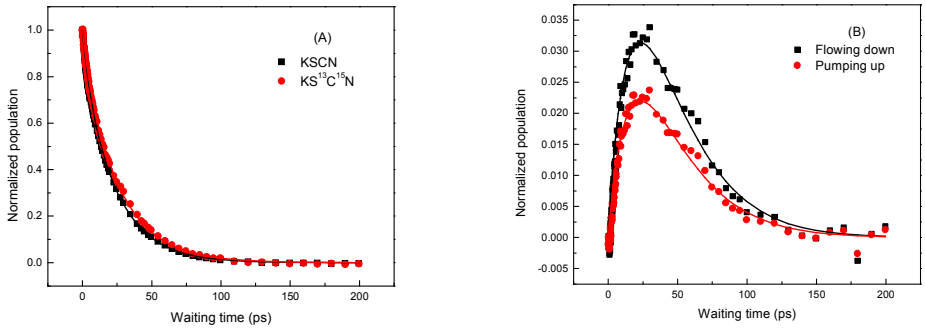

Figure S9. Data and calculations of **Solution J** (NMA:KSCN:$KS^{13}C^{15}N$:D_2O =2:1:1:20). Dots are data, and lines are calculations.

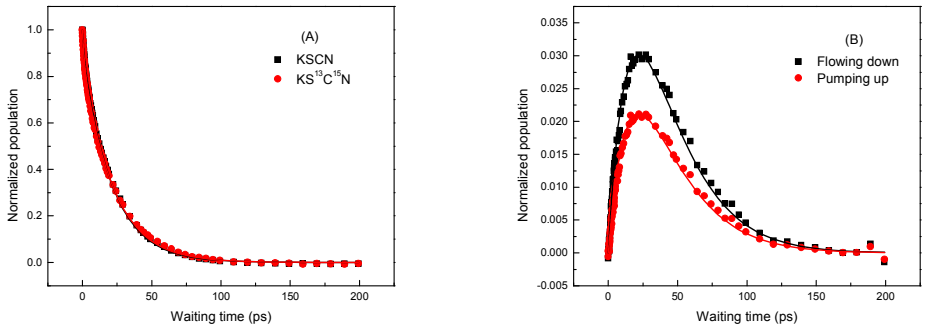

Figure S10. Data and calculations of **Solution K** (NMA:KSCN:$KS^{13}C^{15}N$:D_2O =4:1:1:20). Dots are data, and lines are calculations.

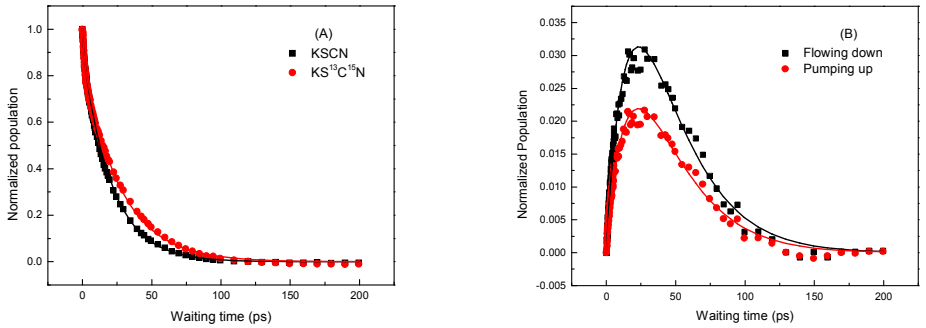

Figure S11. Data and calculations of **Solution L** (Acetone:KSCN:$KS^{13}C^{15}N$:D_2O =2:1:1:20). Dots are data, and lines are calculations.

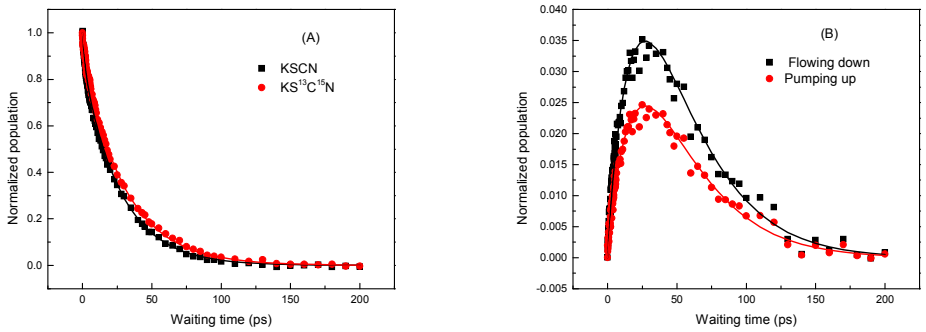

Figure S12. Data and calculations of **Solution M** (DMF:KSCN:$KS^{13}C^{15}N$:D_2O =2:1:1:20). Dots are data, and lines are calculations.

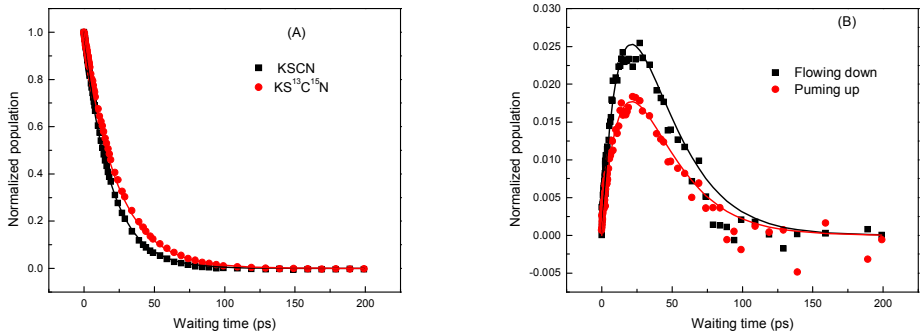

Figure S13. Data and calculations of **Solution N** ($HCONH_2$:KSCN:$KS^{13}C^{15}N$:D_2O =2:1:1:20). Dots are data, and lines are calculations.

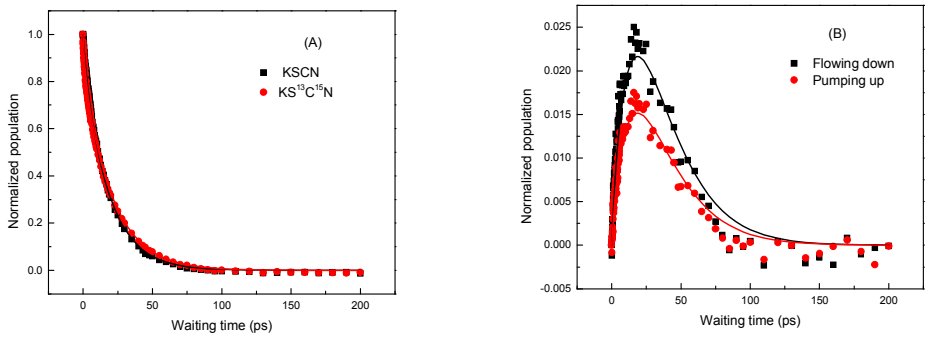

Figure S14. Data and calculations of **Solution O** ($(C_2H_5)_2NH$:KSCN:$KS^{13}C^{15}N$:D_2O =2:1:1:20). Dots are data, and lines are calculations.

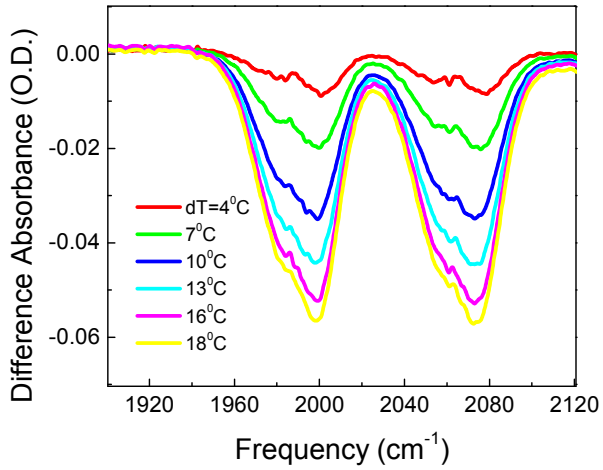

Figure S15. The temperature difference FTIR spectra of the 4M KSCN/KS^{13}C^{15}N=1/1 D_2O solution. Each colored line represents the absorbance difference (high temperature - low temperature) between a measurement at a higher temperature and the measurement at room temperature. Negative value represents bleaching. Heating induces obvious bleachings near the 0-1 transition frequencies (~2066 and 1993 cm^{-1}) of the nitrile stretches. The effect near the 1-2 transition frequencies (~2040 and 1965 cm^{-1}) is much smaller. In 2D IR measurements, the heat from vibrational relaxations increases the temperature of the sample. Because the 2D IR spectra are the difference intensity between experiments with excitation on and off, the heat effect is similar to the temperature difference FTIR spectra shown here. In our setup, the temperature increase from vibrational relaxations is only a few degrees.

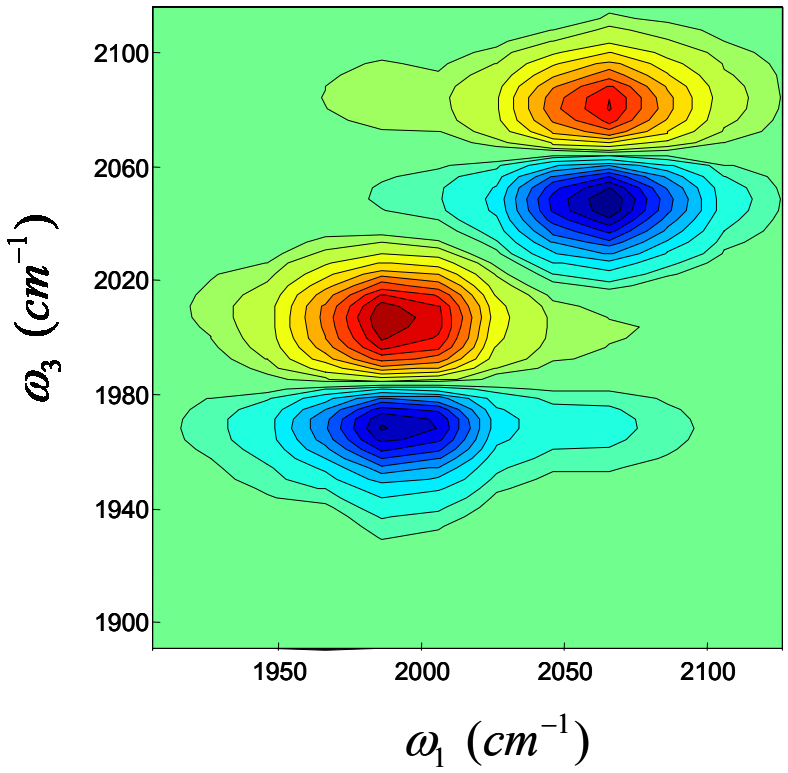

Figure S16. 2D IR spectrum at 30 ps of potassium-H_2O-D_2O (1:1:10) solution. No OH induced heat effect is observed in peaks 5 and 7.

Equilibrium constant calculation

To quantitatively describe the relative binding affinity of the model compounds to the thiocyanate anions, we constructed an equilibrium model to analyze the vibrational energy exchange results. Using **Solution C** as an example, three types of thiocyanate anions coexist under chemical equilibrium: clustered ($SCN^-_{clustered}$), hydrated ($SCN^-_{hydrated}$) and proline-complexed (SCN^-_{pro}). Two types of proline molecules coexist: hydrated ($pro_{hydrated}$) and thiocyanate-complexed (pro_{SCN^-}).We defined these three species based on the experimental observable – vibrational energy transfer: (1) those anions that can transfer energy to other anions are defined as clustered; (2) those anions that can't transfer energy to other anions, which is caused by binding to water, are defined by hydrated; (3) those anions that can't transfer energy, which is caused by binding to model compounds, are defined by compound-complexed. They are not directly related to the physical contact. For example, some water molecules can directly contact S of SCN^-, but these molecules can't block the CN energy transfer. Therefore, these molecules are not considered as those water molecules "hydrate" the SCN^- in the model.

The binding affinity between thiocyanate and proline is defined as

$$K_{affinity} = \frac{\left[SCN^-_{pro}\right]\left[D_2O\right]^n}{\left[SCN^-_{hydrated}\right]\left[pro_{hydrated}\right]}, \qquad \text{Eq.S5}$$

from the following equilibrium,

$$SCN^-_{hydrated} + pro_{hydrated} \rightleftharpoons SCN^-_{pro} + nD_2O\,. \qquad \text{Eq.S6}$$

In the model, we considered the self-associated proline molecules as the hydrated species. The total concentration of water was taken as constant since the amount of

additive is relatively small, leading to a constant concentration of hydrated thiocyanate anions. In this approximation, proline/thiocyanate complexes in both water and ion clusters are mathematically combined into one parameter: SCN^{-}_{pro}. The concentration sum of proline-complexed and hydrated thiocyanate anions was obtained from the vibrational energy exchange experiments, and the concentration of proline was known beforehand. Eq.S6 is readily solvable with all these parameters known. The number of water molecules in Eq.S6 was set to be 1 for comparison of the one-to-one binding affinity.

Using refractive index (table S2) and transition dipole moment correction (table S3), all available $K_{affnity}$ values are listed in Table 1 in the main text and table S4. Two calculations are showed in the following:

Solution B: potassium thiocyanate-proline-D_2O=1-0.5-10. The concentration of potassium is 4M. Cluster ratio is 48%.

$$[\mathrm{SCN^-}]_{total} = 4.00M;[\mathrm{Pro}]_{\mathrm{total}} = 2.00M;$$
$$\Delta\left[\mathrm{SCN^-}\right]_{\mathrm{Cluster}} = \left[\mathrm{SCN^-}\right]_{\mathrm{Pro}} = 4.00 - 1.92 - 1.32 = 0.76\mathrm{M};[\mathrm{D_2O}]_{\mathrm{total}} = 40.00M;$$
$$[\mathrm{D_2O}]_{\mathrm{Pro}} = [\mathrm{Pro}]_{\mathrm{D_2O}} = \left[\mathrm{Pro}\right]_{\mathrm{total}} - [\mathrm{Pro}]_{\mathrm{SCN^-}} = 2.00\text{-}0.76{=}1.24\mathrm{M};[\mathrm{D_2O}]_{\mathrm{Bulk}} = 38.76\mathrm{M};$$
$$\mathrm{K_{affinity}} = \frac{\left[\mathrm{SCN^-}\right]_{\mathrm{Pro}}[\mathrm{D_2O}]_{\mathrm{Bulk}}}{[\mathrm{Pro}]_{\mathrm{D_2O}}[\mathrm{SCN^-}]_{hydrated}} = \frac{0.76\times 38.76}{1.24\times 1.32} = 18.00$$

Solution O: potassium thiocyanate-$(C_2H_5)_2NH$-D_2O=1-1-10. The concentration of KSCN is 4M. Cluster ratio is 52%.

$$[\mathrm{SCN^-}]_{total} = 4.00M;[(\mathrm{C_2H_5})_2\mathrm{NH}]_{\mathrm{total}} = 4.00M;$$
$$\Delta\left[\mathrm{SCN^-}\right]_{\mathrm{Cluster}} = \left[\mathrm{SCN^-}\right]_{(\mathrm{C_2H_5})_2\mathrm{NH}} = 4.00 - 2.08 - 1.32 = 0.60\mathrm{M};[\mathrm{D_2O}]_{\mathrm{total}} = 40.00M;$$
$$[\mathrm{D_2O}]_{(\mathrm{C_2H_5})_2\mathrm{NH}} = [(\mathrm{C_2H_5})_2\mathrm{NH}]_{\mathrm{D_2O}} = \left[(\mathrm{C_2H_5})_2\mathrm{NH}\right]_{\mathrm{total}} - [(\mathrm{C_2H_5})_2\mathrm{NH}]_{\mathrm{SCN^-}} = 4.00\text{-}0.60{=}3.40\mathrm{M};[\mathrm{D_2O}]_{\mathrm{Bulk}} = 36.60\mathrm{M};$$
$$\mathrm{K_{affinity}} = \frac{\left[\mathrm{SCN^-}\right]_{(\mathrm{C_2H_5})_2\mathrm{NH}}[\mathrm{D_2O}]_{\mathrm{Bulk}}}{[(\mathrm{C_2H_5})_2\mathrm{NH}]_{\mathrm{D_2O}}[\mathrm{SCN^-}]_{hydrated}} = \frac{0.60\times 36.60}{3.40\times 1.32} = 4.89$$

Table S1. Cluster ratios of different samples before IR cross section and refractive index corrections

Samples	Cluster ratio
Solution A	**67%±2%**
Solution B	**48%±4%**
Solution C	**34%±5%**
Solution D	**45%±4%**
Solution E	**38%±5%**
Solution F	**30%±7%**
Solution G	**65%±4%**
Solution H	**46%±4%**
Solution J	**56%±4%**
Solution K	**50%±4%**
Solution L	**64%±4%**
Solution M	**61%±4%**
Solution N	**51%±4%**
Solution O	**52%±4%**

Solution A (Pro:KSCN:$KS^{13}C^{15}N$:D_2O =0:1:1:20);
Solution B (Pro:KSCN:$KS^{13}C^{15}N$:D_2O =1:1:1:20);
Solution C (Pro:KSCN:$KS^{13}C^{15}N$:D_2O =2:1:1:20);
Solution D (Gly:KSCN:$KS^{13}C^{15}N$:D_2O=1:1:1:20);
Solution E (Cys:KSCN:$KS^{13}C^{15}N$:D_2O =1:1:1:20);
Solution F (Lys:KSCN:$KS^{13}C^{15}N$:D_2O =1:1:1:20);
Solution G (CH_3COOK:KSCN:$KS^{13}C^{15}N$:D_2O =2:1:1:20);
Solution H (CH_3NH_3Cl:KSCN:$KS^{13}C^{15}N$:D_2O =1:1:1:20);
Solution J (NMA:KSCN:$KS^{13}C^{15}N$:D_2O =2:1:1:20);
Solution K (NMA:KSCN:$KS^{13}C^{15}N$:D_2O =4:1:1:20);
Solution L (Acetone:KSCN:$KS^{13}C^{15}N$:D_2O =2:1:1:20);
Solution M (DMF:KSCN:$KS^{13}C^{15}N$:D_2O =2:1:1:20);
Solution N ($HCONH_2$:KSCN:$KS^{13}C^{15}N$:D_2O =2:1:1:20);
Solution O ($(C_2H_5)_2NH$:KSCN:$KS^{13}C^{15}N$:D_2O =2:1:1:20);

Local refractive index corrections

As mentioned in the main text, adding another species into the potassium thiocyanate aqueous solutions will inevitably change the refractive indexes of the solutions and the transition dipole moments of the nitrile stretches if the additives can interact with the thiocyanate anions. According to the vibrational energy transfer equation and the dipole/dipole approximation, shown in Eq.S7&S8, these two factors can also affect the vibrational energy transfer rates, in addition to the ion cluster concentration:

$$k_{DA} = \frac{1}{1+e^{-\frac{\Delta\omega_{DA}}{RT}}}\langle\beta\rangle^2 \frac{\frac{1}{\tau_c}}{(\frac{1}{\tau_c})^2 + (\Delta\omega_{DA})^2}, \qquad \text{Eq.S7}$$

where k_{DA} is the energy transfer rate constant from the donor (D) to the acceptor (A). $\Delta\omega_{DA} = \omega_D - \omega_A$ is the frequency difference between the donor and the acceptor. R is the gas constant. T is the temperature. $\langle\beta\rangle$ is the average coupling constant between D and A. τ_c is the coupling fluctuation time. For all the room temperature liquids we studied so far, τ_c was found to be $2.0 \pm 0.1 ps$. This is at the same time scale as that of solvent molecules reorganizing their configurations, corresponding to the molecular binding enthalpy ~0.6 kcal/mol which is the same as the thermal energy at room temperature. $(\frac{1}{\tau_c})^2$ is in the energy or frequency unit corresponding to each τ_c.

The coupling between two dipoles is given by

$$\langle\beta\rangle = \frac{1}{4\pi\varepsilon_0 n^2}\left[\frac{\boldsymbol{\mu}_D\cdot\boldsymbol{\mu}_A}{r_{DA}^3} - 3\frac{(\boldsymbol{\mu}_D\cdot\mathbf{r}_{DA})(\boldsymbol{\mu}_A\cdot\mathbf{r}_{DA})}{r_{DA}^5}\right] = \frac{1}{4\pi\varepsilon_0 n^2}\frac{\mu_D\mu_A\kappa}{r_{DA}^3}, \quad \text{Eq.S8}$$

where ε_0 is vacuum permittivity, n is the local refractive index of the media, $\kappa = \cos\theta_{DA} - 3\cos\theta_D\cos\theta_A$, θ_{AD} is the angle between the two transition dipole moments and θ_A and θ_D are the angles between each transition moment and the vector connecting them. $\boldsymbol{\mu}_D$ and $\boldsymbol{\mu}_A$ are the transition dipole moments of donor and acceptor, respectively. r_{DA} is the distance between the donor and acceptor.

Therefore, the variations of transition dipole moments and local refractive indexes induced by the additions of molecules need to be corrected before the concentration of clustered ions can be finally obtained from the energy transfer measurements.

The refractive indexes of KSCN/D_2O (1/10, 4M), (1/7.5, ~5M) and (1/5, 6.5M) solutions were calculated to be 1.41, 1.43, and 1.46 respectively, according to literature.[3] We used Eq. S9&S10 to estimate the refractive indexes of solutions with different model compounds with a molecule/salt/water molar ratio 1/1/10:

$$n_{sol} = 1.41 + 0.05\times\frac{n_{compound} - 1.41}{n_{KSCN} - 1.41}, \quad \text{Eq.S9}$$

and another equation for solutions with compounds with molecule/salt/water molar ratio 0.5/1/10:

$$n_{sol} = 1.41 + 0.02\times\frac{n_{compound} - 1.41}{n_{KSCN} - 1.41}. \quad \text{Eq.S10}$$

The refractive index of KSCN at 5 microns is 1.53. For most of the compounds, the refractive indexes at 5 microns are not available from literature. Instead, we use the values at ~600nm reported in references [4-10]. In these compounds, refractive index of

the NH_3CH_3Cl is not available. We took the value 1.44 that comes from the compound $NH_2(CH_3)_2Cl$ instead. This can cause about 0.5% - 1% uncertainty (estimated from the frequency dependent of refractive indexes of KI, KF, NaCl) in the final results. Corrected results are displayed in table S2. The refractive index changes are smaller than 1.5%, within this range: 1.41 ± 0.2, except for the KSCN:Pro:D_2O= 1:1:10 of which n = 1.44.

Table S2. Refractive indexes of solutions

	Refractive index (pure compound)	Sample	Refractive index (solution)
Glycine	1.500	KSCN:Gly:D_2O= 0.5:1:10	1.42
Proline	1.487	KSCN:Pro:D_2O =0.5:1:10 KSCN:Pro:D_2O= 1:1:10	1.42 1.44
Lysine	1.503	KSCN:Lys:D_2O =0.5:1:10	1.43
NMA	1.428	KSCN:NMA:D_2O= 1:1:10 KSCN:NMA:D_2O= 2:1:10	1.41 1.42
Formamide	1.447	KSCN:FMA:D_2O =0.5:1:10	1.42
CH_3COOK	1.370	KSCN:Ack:D_2O =1:1:10	1.39
Acetone	1.360	KSCN:Acetone:D_2O= 1:1:10	1.39
Diethylamide	1.385	KSCN:DAM:D_2O =1:1:10	1.40
DMF	1.431	KSCN:DMF:D_2O =1:1:10	1.42
Diethylamine	1.385	KSCN: DEA :D_2O= 1:1:10 KSCN: DEA :D_2O= 1:1:10	1.41 1.40
NH_3CH_3Cl	1.44	KSCN:NH_3CH_3Cl:D_2O=1:0.5:10	1.42

Transition dipole moment correction

The nitrile stretch 0-1 transition dipole moment changes induced by the addition of model compounds were determined in the following procedure. A model compound and water were mixed with a certain molar ratio to match that of the sample in 2D IR measurements. FTIR spectrum was taken from this mixture as the background. KSCN was then added into the mixture with a molar ratio 1/200 (KSCN/water). FTIR spectra of this sample and a solution KSCN/water (=1/200) were then measured. The density of each sample was measured to normalize the number of KSCN in the optical path. The change of the CN transition dipole moment square is then proportional to the intensity change of CN stretch peak 2065 cm^{-1} between with and without the model compound. The uncertainty of the measurements was estimated to be ~5%. The change given by this method is the maximum change the nitrile stretch can have. In the 2D IR samples, because the KSCN concentration is much higher, the change is expected to be smaller. At the concentrations of 2D IR samples, the FTIR measurements could not be reliably repeated because of the very small optical path, 1~2 microns. The measured values of $(\frac{\mu_{mixture}}{\mu_{KSCN}})^2$ are listed in table S3. The transition dipole moments in most mixtures are smaller than that of the KSCN solution for less than 10%.

Table S3. Transition dipole changes

Samples	$(\frac{\mu_{mixture}}{\mu_{KSCN}})^2$
KSCN:Proline:H_2O=0.5:1:10	0.98
KSCN:Proline: H_2O =1.0:1:10	0.91
KSCN:Cysteine: H_2O =0.5:1:10	0.92
KSCN:Glycine: H_2O =0.5:1:10	0.92
KSCN:Lysine: H_2O =0.5:1:10	0.85
KSCN:NMA: H_2O =1:1:10	0.92
KSCN:NMA: H_2O =2:1:10	0.90
KSCN:Acetone: H_2O =1:1:10	1.05
KSCN:Formamide: H_2O =0.5:1:10	0.98
KSCN:diethylamide: H_2O =1:1:H_2O	1.02
KSCN:DMF: H_2O =1:1:10	0.97
KSCN:AcK: H_2O =1:1:10	0.93
KSCN:NH_3CH_3Cl: H_2O =1:1:10	0.91

Corrections for transition dipole moment and local refractive index

Eq.S7&S8 can be simplified as

$$k_{DA} \propto \frac{\mu_D^2 \mu_A^2}{n^4} = \frac{\mu_{CN}^4}{n^4}. \qquad \text{Eq.S11}$$

The change of refractive index is small (<2%). It does not induce a big uncertainty to use the estimated average refractive indexes in table S2 to calculate k_{DA}. However, it can be problematic if the average transition moment changes in table S3 are used because the transition dipole moment changes can be big, up to 10%. Assuming that the transition dipole moment change induced by the addition of a compound is due to the dipole/dipole interaction, this effect is a very short range interaction. According to the dipole/dipole interaction equation Eq.S8, the compound will have very little effect on SCN^- anions which are separated away from this model compound by one other molecule or anion. This situation means that for those SCN^- anions of which the energy exchange can produce visible cross peaks in 2D IR measurements are hardly affected by the addition of the model compound, because they don't directly contact the model compound. Now this will create an interesting situation in the 2D IR spectra. The diagonal peaks are from all SCN^- anions, so that their signals are proportional to the fourth power of the measured average transition dipole moment. However, the cross peaks will be proportional to the fourth power of the transition dipole moment of the clustered anions of which the transition dipole moment is hardly affected by the model compound. The proper kinetic analysis requires the normalization for the difference of transition dipole moments. In reality, it is quite possible that the clustered anions can also be affected by the model compound with a smaller effect. We tested two models to

do the correction: 1. the transition dipole moment of clustered anions is not affected by the addition of a model compound. The peak intensities were renormalized and the calculated cluster concentration and affinity values are listed in table S4. 2. The transition dipole moment of the clustered anions is affected by the addition of a model compound, and the effect is 50% of the measured average effect. The peak intensities were then renormalized accordingly and the energy transfer rate was also normalized with this transition dipole moment change. The calculated cluster concentration and affinity values are listed in table S4. We believe that the 2nd treatment is closer to the real situation and the results are reported, but both treatments give essential the same conclusion.

Table S4. Corrected affinities with method 1&2 and refractive index

	Original concentration	Original affinity	concentration Corrected	Affinity corrected
Pro:KSCN:D_2O 0.5:1:10	48%	18	Method 1: 44% Method 2: 44%	25.1 25.1
Pro:KSCN: D_2O 1:1:10	34%	14	Method 1: 29% Method 2: 35%	17.4 13.3
Gly:KSCN: D_2O 0.5:1:10	45%	23	Method 1: 38% Method 2: 44%	41.0 25.1
Cys:KSCN: D_2O 0.5:1:10	38%	41	Method 1: 31% Method 2: 35%	76.8 52.9
Lys:KCN: D_2O 0.5:1:10	30%	85	Method 1: 24% Method 2: 32%	185 69.6
AcK:KSCN: D_2O 1:1:10	65%	1	Method 1: 55% Method 2: 62%	3.8 1.4
CH_3NH_3Cl:KSCN: D_2O 0.5:1:1	46%	21	Method 1: 38% Method 2: 44%	40.9 25.1
NMA:KSCN: D_2O 1:1:10	56%	3.5	Method 1: 50% Method 2: 58%	5.7 2.7
Acetone:KSCN: D_2O 1:1:10	64%	1	Method 1: 66% Method 2: 62%	0.3 1.4
DMF:KSCN: D_2O 1:1:10	61%	2	Method 1: 56% Method 2: 58%	3.4 2.7
DEA:KSCN: D_2O 1:1:10	52%	5	Method 1: 55% Method 2: 52%	3.8 4.9
FMA:KSCN: D_2O 1:1:10	51%	5	Method 1: 49% Method 2: 52%	6.1 4.9

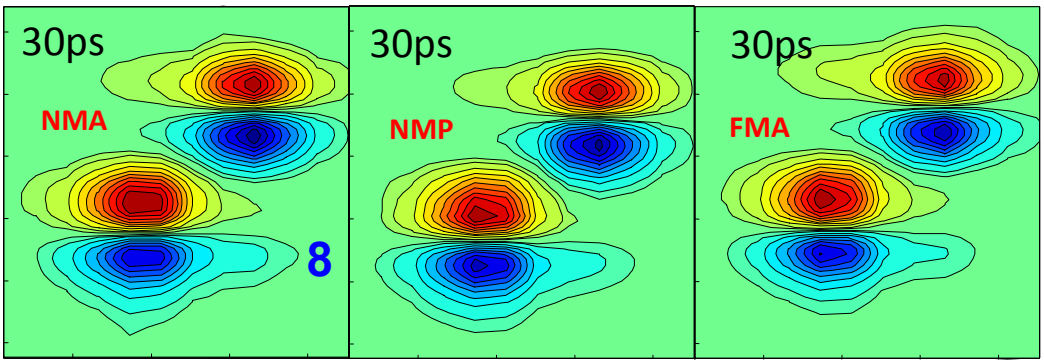

Figure S17. 2D IR spectra at 30 ps of potassium aqueous solutions with the same amount of model compounds: NMA ($CH_3CONHCH_3$), NMP ($HCONHCH_3$), and FMA ($HCONH_2$). With the number of CH_3 group decreasing, the intensity of peak 8 also decreases, indicating the insignificance of the CH_3 group binding to the anion. We also notice that beside the N-H group, the amide bond (CO-N) also plays a role in binding to the anion, as shown in the quantitative analyses in Table S1.

The coupling orientation of KSCN-$HCOND_2$ dimmer

The coupling orientation factor between two modes can be estimated from the DFT calculation results for the dimmers based on Eq. S8. In the orientation factor calculations, the r_{DA} starting point of the CN stretch of SCN^- is the center of the CN bond, and that of the ND stretch of $HCOND_2$ is the position of nitrogen, and that of the OD stretch of D_2O is the position of oxygen. Calculations for isolated molecules and solvated molecules give: $\left(\frac{\kappa_{mean}^{CN/ND}}{\kappa_{mean}^{CN/OD}}\right)_{isolated} = 0.98$, and $\left(\frac{\kappa_{mean}^{CN/ND}}{\kappa_{mean}^{CN/OD}}\right)_{CPCM} = 0.98$. Deatiled parameters are provided in table S5. In estimating the energy transfer rate ratio, the refractive indexes of both solutions were taken to be the same.

Table S5. The calculated coupling orientation factors between different modes in four different samples.

sample	mode	method	θ_D (degree)	θ_A (degree)	θ_{DA} (degree)	κ	κ_{mean}
KSCN/ D_2O	$CN/OD_{stretch}$	Isolated	7.50	3.48	11.0	1.99	1.99
		CPCM	2.79	0.633	3.31	2.00	2.00
KSCN/ $HCOND_2$	$CN/ND_{stretch}$	Isolated	4.18	9.15	4.97	1.96	1.96
		CPCM	0.0674	13.3	13.2	1.95	1.95

References

1. Bian, H. T.; Chen, H. L.; Li, J. B.; Wen, X. W.; Zheng, J. R. *J. Phys. Chem. A* **2011**, *115*, 11657-11664.
2. Bian, H. T.; Wen, X. W.; Li, J. B.; Chen, H. L.; Han, S. Z.; Sun, X. Q.; Song, J. A.; Zhuang, W.; Zheng, J. R. *Proc. Natl. Acad. Sci. U. S. A.* **2011**, *108*, 4737-4742.
3. Bostrom, M.; Williams, D. R. M.; Ninham, B. W. *Biophys. J.* **2003**, *85*, 686-694.
4. Orttung, H. W.; Armour, W. R. *J. Phys. Chem.* **1967**, *71*, 2846-2853.
5. Lacourt, A.; Delande, N.; Depaduwa, G. *Anal. Chim. Acta* **1956**, *14*, 100-108.
6. Resa, J. M.; Gonzalez, C.; Landaluce, S. O.; Lanz, J. *J Chem. Eng. Data* **2000**, *45*, 867-871.
7. Abdel-Azim, Abdel-Azim A.; Munk, P. *J. Phys. Chem.* **1987**, 91, 3910 - 3914.
8. Checoni, F. R.; Volpe, L. O. P. *J. Solu. Chem.* **2010**, *39*, 259 - 276.
9. Gill, K.B.; Rattan, K.V.; Kapoor, S. *J. Chem. Eng. Data* **2009**, *54*, 1175 - 1178.

10. Popova, S. A.; Orlova, V. T.; Borina, A. F. *Russ. J. Inorg. Chem.* **1993**, *38*, 665-669.